Research Article

Elkhateeb Sobhy Aly*, Manoj Singh, Mohammed Ali Aiyashi, and Mohammed Daher Albalwi

Modeling monkeypox virus transmission: Stability analysis and comparison of analytical techniques

https://doi.org/10.1515/phys-2024-0056
received December 22, 2023; accepted June 20, 2024

Abstract: Monkeypox is a highly infectious disease and spreads very easily, hence posing several health concerns or risks as it may lead to outbreak. This article proposes a new mathematical model to simulate the transmission rate of the monkeypox virus-infected fractional-order differential equations using the Caputo–Fabrizio derivative. The existence, uniqueness, and stability under contraction mapping of the fixed point of the model are discussed using Krasnoselskii's and Banach's fixed point theorems. To verify the model proposed, we employ data that record the actual dynamics, and based on these data, the model can capture the observed transmission patterns in Ghana. Also, the analytic algorithm is used to find the result applying the Laplace Adomian decomposition method (LADM). Performance analysis of LADM is made regarding Runge-Kutta fourth order, which is the most commonly employed method for solving second-order ordinary differential equations. This comparison therefore offers information on the truth and reliability of the two techniques toward modeling the transmission pattern of the monkey pox virus. The information obtained through this study provides a better understanding of the antibodies linked to monkeypox virus spreading and provides effective strategies to doctors and politicians. This article helps shape better strategies about combating the impact of monkeypox virus in public health since it makes it easy to predict and prevent the occurrence of the disease.

Keywords: monkeypox virus, stability analysis, Caputo–Fabrizio derivative, Krasnoselskii's and Banach's fixed point

1 Introduction

Fractional calculus is thus a phenomenon that has gained attention also by helping model biological systems, bringing a more sophisticated view of biological entities and their memory-based processes. While integer-order derivatives are restrictive in addressing the kind of dynamic, anomalous diffusion, and correlation, which are characteristic of a biological system, fractional derivatives offer a much more flexible way to address these issues. Through the use of fractional calculus for modeling in biological systems, scientists and researchers can describe various dynamics that have not been previously modeled effectively, including infection spread, cellular division, and neural firing [1–6]. This improved modeling ability provides a basic understanding of the forces at the core of such processes and also provides more accurate prediction of results [7,8]. Thus, fractional calculus not only enriches our understanding of biological oscillations and chaotic phenomena but also contributes toward the techniques of disease prevention and cure, prevention strategy of diseases, and biological resource conservation [9–14].

Scientists have been looking at the rapid appearance and global spread of monkeypox in the middle of the continuing Coronavirus Disease 2019 (COVID-19) pandemic. As of June 22, 2022, 3,340 confirmed cases of the most significant and most prevalent monkeypox epidemic outside of Africa have been documented around the globe. Monkeypox may be passed from one person to another by vertical transmission from mother to child and through contact with infected skin or mucosal skin sores, respiratory droplets, or contaminated items or materials [15–19]. The monkeypox virus is a

*** Corresponding author: Elkhateeb Sobhy Aly,** Department of Mathematics, Faculty of Science, Jazan University, P.O. Box 114, Jazan 45142, Saudi Arabia; Nanotechnology Research Unit, College of Science, Jazan University, P.O. Box 114, Jazan 45142, Saudi Arabia, e-mail: elkhateeb@jazanu.edu.sa
Manoj Singh: Department of Mathematics, Faculty of Science, Jazan University, P.O. Box 114, Jazan 45142, Saudi Arabia, e-mail: msingh@jazanu.edu.sa
Mohammed Ali Aiyashi: Department of Mathematics, Faculty of Science, Jazan University, P.O. Box 114, Jazan 45142, Saudi Arabia, e-mail: maiyashi@jazanu.edu.sa
Mohammed Daher Albalwi: Yanbu Industrial College, The Royal Commission for Jubail and Yanbu, 30436, Jubail, Saudi Arabia, e-mail: albalwim@rcjy.edu.sa

member of the Chordopoxvirinae subfamily of the Poxviridae family of enclosed, linear, double-stranded DNA viruses. Monkeypox is typically a self-limiting illness, with symptoms typically lasting between 2 and 4 weeks and a historical fatality rate of 0–11. Monkeypox may cause severe headaches, fever, skin lesions, and lymphadenopathy. Despite the lack of a particular therapy or vaccine for monkeypox virus infection, antiviral drugs and smallpox vaccinations have been licensed for use in several countries in response to the epidemic. Rapid intervention is needed before the virus can effectively establish person-to-person transmission, leading to a worldwide monkeypox pandemic [20–29].

After smallpox was abolished, monkeypox emerged as the dominant pox in humans. The transmission of an epidemic is currently considered quite unlikely [30,31]. Humans can get the illness by close contact with an infected animal or person or contact with contaminated materials. The virus has been shown to spread from person to person in the United Kingdom [32] and the Democratic Republic of the Congo [33]. Thornhil et al. [34] found that among 528 people with the disease from 16 countries, 98% identified as homosexual. A number of cases of monkeypox were recorded in Ghana on May 24, 2022 [35]. The World Health Organization classified monkeypox as a developing moderate public health concern threat on June 23, 2022. Since September 2022, there have been over 65,000 confirmed instances of monkeypox virus infection throughout 106 nations and 5 geographical zones, with 26 fatalities. The current global outbreak of monkeypox virus infection in humans may be caused by a combination of factors, including waning smallpox immunity, relaxing COVID-19 prevention measures, resuming international travel, and sexual interactions associated with large gatherings [34]. Few investigations on disease transmission have been conducted in the past [36–38]. However, mathematical models have been used to investigate the information of diseases such as COVID-19 [39,40] and Poxviridae diseases such as smallpox [41–43], chickenpox [44,45], and cowpox [46].

Moreover, in monkeypox virus research, Peter et al. [36] conducted a ground-breaking study using actual data from Nigeria to investigate the virus's transmission dynamics using the innovative concepts of fractional calculus. Their investigation intended to shed light on the complex modeling system and its implications for infection control policies, providing the general public with crucial insights regarding the importance of control parameters in eradicating the virus from the studied population. Peter et al. [38] took a mathematical modeling approach to elucidate additional aspects of the virus's transmission dynamics, building on their pioneering work. Isolating infected individuals from the general population effectively reduces disease transmission, as revealed by their research, which holds tremendous promise for regulating the spread of the virus. This discovery offers a compelling intervention strategy that can play a crucial role in preventing the spread of the virus and protecting public health. By continuously pushing the limits of mathematical modeling, these studies substantially contribute to ongoing efforts to combat the monkeypox virus, offering hope and opportunities for more effective control and prevention measures.

In the recent analysis of the dynamics of infectious diseases especially those involving spread of highly transmissible viruses such as monkeypox, incorporation of sophisticated modeling and computations is a new and significant innovation. This article aims at presenting a unique model that is specifically designed to help investigate the complex transmission of monkeypox virus. Different from traditional models, our proposed approach employs a certain type of derivative called Caputo–Fabrizio derivative, which enhances the description of the disease progression and transmission rate. Furthermore, we utilize a fresh approach involving Krasnoselskii's and Banach's fixed point theorems with a view of analyzing the stability properties of the model and gain insights into the spread of viruses. Furthermore, our study presents the novel approach of using the Laplace Adomian decomposition method (LADM) to obtain the approximate solution of the model and enhance the understanding of the characteristics of the system and some important control strategies. Therefore, applying these new mathematical methods alongside actual data from Ghana not only proves the usefulness of the model in its ability to simulate observed rates of transmission but will also serve as a strong framework for policy makers and managers in the health sector to work toward the prevention and control of monkeypox.

2 Mathematical modeling

We attempt to construct an advanced mathematical model by analyzing the foundations set out in the study of Peter et al. [38] using a novel approach. Using the existing framework as a foundation, we aim to improve its efficacy by incorporating an additional dimension that accounts for virus-immune individuals. This modification permits us to understand the complex dynamics of virus transmission from person to person, taking into account the impact of immunity. To achieve this, we divide the population into six distinct compartments, each representing a distinct state: susceptible individuals, denoted by W_S; exposed individuals, denoted by W_E; infected individuals, denoted by W_A; hospitalization-required individuals, denoted by W_Q; recovered individuals, denoted by W_R; and highly immune

individuals, denoted by W_V. The total population is elegantly represented by the equation $N(t) = W_S + W_E + W_A + W_Q + W_R + W_V$, where t is a time variable. This mathematical model can potentially unravel the complex dynamics of the monkeypox virus's propagation, providing invaluable insights into how it affects population susceptibility, exposure, immunity, and recovery:

$$\begin{cases} \dfrac{dW_S(t)}{dt} = \omega - \omega_2 \dfrac{W_A W_S}{N} - \omega_1 W_S, \\ \dfrac{dW_E(t)}{dt} = \omega_2 \dfrac{W_A W_S}{N} - (\omega_7 + \omega_1) W_E, \\ \dfrac{dW_A(t)}{dt} = \omega_7 W_E - (\omega_1 + \omega_3 + \omega_4 + \omega_5) W_A, \\ \dfrac{dW_Q(t)}{dt} = \omega_4 W_A - (\omega_1 + \omega_5 + \omega_6) W_Q, \\ \dfrac{dW_R(t)}{dt} = \omega_6 W_Q + \omega_3 W_A - \omega_1 W_R, \\ \dfrac{dW_V(t)}{dt} = \omega\eta - \omega_1 W_V, \end{cases} \tag{1}$$

subject to the initial conditions

$$W_S(0) = W_{S,0}, \quad W_E(0) = W_{E,0}, \quad W_A(0) = W_{A,0},$$
$$W_Q(0) = W_{Q,0}, \quad W_R(0) = W_{R,0}, \quad \text{and} \quad W_V(0) = W_{V,0}.$$

To achieve a more accurate and exhaustive depiction of the phenomenon, we drew inspiration from Caputo's pioneering works [47–50]. By maintaining a constant dimension on both sides of the system, we ensured our strategy's consistency and validity. As a result, the fractional Liouville–Caputo derivative of the monkeypox disease system is determined, constituting a crucial component of our analytical model. Notably, the model under consideration, denoted by (1), is expressed as a Caputo-type derivative, providing a solid basis for understanding and analyzing the complex dynamics of monkeypox spread. This novel approach promises to yield significant insights into the disease's underlying transmission mechanisms and can aid in developing effective control and prevention strategies. Caputo's influential works [47–50], which serve as the foundation of our research framework, are acknowledged and cited by stringent academic integrity standards throughout this study:

$$\begin{cases} D_t^{\mu} W_S(t) = \omega - \omega_2 \dfrac{W_A W_S}{N} - \omega_1 W_S, \\ D_t^{\mu} W_E(t) = \omega_2 \dfrac{W_A W_S}{N} - (\omega_7 + \omega_1) W_E, \\ D_t^{\mu} W_A(t) = \omega_7 W_E - (\omega_1 + \omega_3 + \omega_4 + \omega_5) W_A, \\ D_t^{\mu} W_Q(t) = \omega_4 W_A - (\omega_1 + \omega_5 + \omega_6) W_Q, \\ D_t^{\mu} W_R(t) = \omega_6 W_Q + \omega_3 W_A - \omega_1 W_R, \\ D_t^{\mu} W_V(t) = \omega\eta - \omega_1 W_V, \end{cases} \tag{2}$$

subject to the initial conditions

$$W_S(0) = W_{S,0}, \quad W_E(0) = W_{E,0}, \quad W_A(0) = W_{A,0},$$
$$W_Q(0) = W_{Q,0}, \quad W_R(0) = W_{R,0}, \quad \text{and} \quad W_V(0) = W_{V,0},$$

where μ shows that fractional-order, $0 < \mu \leq 1$ and t is the defined time. Fractional calculus has recently gained significant popularity as a practical and efficient way to approximate real-world situations. Because of its ability to clarify complex dynamic systems with memory effects, it is helpful in a wide range of fields, including biology, mathematics, engineering, finance, economics, and the social sciences. To fully capture memory effects, several major fractional derivatives have been created, especially in solving a wide range of human health issues. The Caputo fractional derivative is a novel formulation that has gained extensive use in simulating various application models. The proposed model's flowchart is shown in Figure 1.

3 Basic definitions

In the subject of this research, we want to define several important concepts, such as:

Definition 1. Suppose Υ belongs to $\mathcal{H}^1(a, b)$, where $b > a$, and $\mu \in (0, 1)$. Under these conditions, the provided Caputo-Fabrizio fractional derivative (CFFD) is as follows [51]:

$${}^{CF}_{0}D_t^{\mu}\Upsilon(t) = \frac{\mathcal{K}(\mu)}{1-\mu}\int_a^t \Upsilon'(\Theta)\exp\left[-\frac{t-\Theta}{1-\Theta}\right]d\Theta. \tag{3}$$

Given that $\mathcal{K}(\mu)$ in (3) adheres to the conditions $\mathcal{K}(1) = \mathcal{K}(0) = 1$, if Υ does not belong to $\mathcal{H}^1(a, b)$, the equation transforms to [51]:

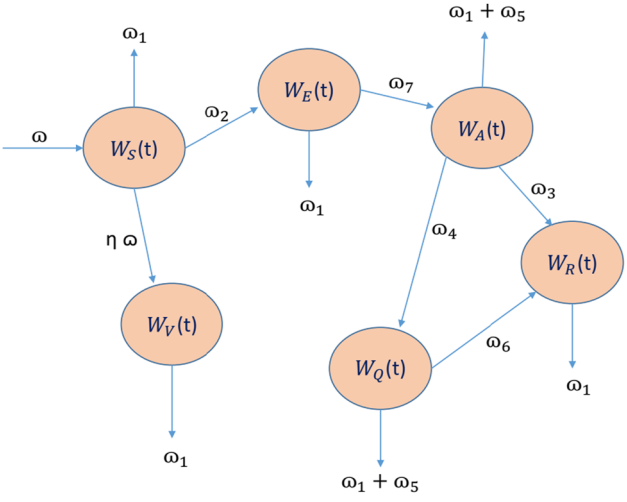

Figure 1: Flowchart of the proposed model.

$$ {}^{\mathrm{CF}}_{0}D_t^{\mu}\Upsilon(t) = \frac{\mathcal{K}(\mu)}{1-\mu}\int_{\alpha}^{t}\Upsilon(t) - \Upsilon(\Theta)\exp\left[-\frac{t-\Theta}{1-\Theta}\right]\mathrm{d}\Theta. $$

Definition 2. Suppose $\mu \in (0,1]$; then, the fractional-order integral of the function Υ is represented as [51]:

$$ {}^{\mathrm{CF}}_{0}I_t^{\mu}\Upsilon(t) = \frac{(1-\mu)}{\mathcal{K}(\mu)}\Upsilon(t) + \frac{\mu}{\mathcal{K}(\mu)}\int_{0}^{t}\Upsilon(\Theta)\mathrm{d}\Theta. $$

Lemma 1. *The problem arising from CFFD lies in the fact that* [51]

$$ \begin{cases} {}^{\mathrm{CF}}_{0}D_t^{\mu}\Upsilon(t) = z(t), & 0 < \mu \le 1, \\ \Upsilon(0) = \Upsilon_0, & \textit{where } \Upsilon \textit{ is real constant}. \end{cases} $$

Alternatively, it can be expressed as the integral:

$$ \Upsilon(t) = \Upsilon_0 + \frac{1-\mu}{\mathcal{K}(\mu)}\Upsilon(t) + \frac{\mu}{\mathcal{K}(\mu)}\int_{0}^{t}\Upsilon(\Theta)\mathrm{d}\Theta. $$

Definition 3. [52,53] The Laplace transform of CFFD, denoted as ${}^{\mathrm{CF}}_{0}D_t^{\mu}$ with $\mu \in (0,1]$ of $M(t)$, is expressed as

$$ L[{}^{\mathrm{CF}}_{0}I_t^{\mu}M(t)] = \frac{sL[M(t)] - M(0)}{s + \mu(1-s)}. $$

4 Monkeypox virus fractional-order modeling: findings on existence and uniqueness

We utilize Banach's and Krassnolsekii's theorems to demonstrate at least one solution to the model:

$$ \begin{cases} f_1(t, W_S, W_E, W_A, W_Q, W_R, W_V) \\ = \omega - \omega_2\dfrac{W_A W_S}{N} - \omega_1 W_S, \\ f_2(t, W_S, W_E, W_A, W_Q, W_R, W_V) \\ = \omega_2\dfrac{W_A W_S}{N} - (\omega_7 + \omega_1)W_E, \\ f_3(t, W_S, W_E, W_A, W_Q, W_R, W_V) \\ = \omega_7 W_E - (\omega_1 + \omega_3 + \omega_4 + \omega_5)W_A, \\ f_4(t, W_S, W_E, W_A, W_Q, W_R, W_V) \\ = \omega_4 W_A - (\omega_1 + \omega_5 + \omega_6)W_Q, \\ f_5(t, W_S, W_E, W_A, W_Q, W_R, W_V) \\ = \omega_6 W_Q + \omega_3 W_A - \omega_1 W_R, \\ f_6(t, W_S, W_E, W_A, W_Q, W_R, W_V) \\ = \omega\eta - \omega_1 W_V, \end{cases} \tag{4} $$

where

$$ W_S(0) = P_1, \quad W_E(0) = P_2, \quad W_A(0) = P_3, \quad W_Q(0) = P_4, $$
$$ W_R(0) = P_5, \quad \text{and} \quad W_V(0) = P_6. $$

Consequently, our problem transforms to

$$ \begin{cases} \mathrm{D}_t^{\mu}W_S = f_1(t, W_S, W_E, W_A, W_Q, W_R, W_V), \\ \mathrm{D}_t^{\mu}W_E = f_2(t, W_S, W_E, W_A, W_Q, W_R, W_V), \\ \mathrm{D}_t^{\mu}W_A = f_3(t, W_S, W_E, W_A, W_Q, W_R, W_V), \\ \mathrm{D}_t^{\mu}W_Q = f_4(t, W_S, W_E, W_A, W_Q, W_R, W_V), \\ \mathrm{D}_t^{\mu}W_R = f_5(t, W_S, W_E, W_A, W_Q, W_R, W_V), \\ \mathrm{D}_t^{\mu}W_V = f_6(t, W_S, W_E, W_A, W_Q, W_R, W_V), \end{cases} \tag{5} $$

where

$$ W_S(0) = P_1, \quad W_E(0) = P_2, \quad W_A(0) = P_3, \quad W_Q(0) = P_4, $$
$$ W_R(0) = P_5, \quad \text{and} \quad W_V(0) = P_6. $$

Let

$$ \hbar(t) = \begin{bmatrix} W_S \\ W_E \\ W_A \\ W_Q \\ W_R \\ W_V \end{bmatrix}, \hbar_0 = \begin{bmatrix} P_1 \\ P_2 \\ P_3 \\ P_4 \\ P_5 \\ P_6 \end{bmatrix}, \quad \text{and} \quad F(t, \hbar(t)) = \begin{bmatrix} f_1(t, \hbar(t)) \\ f_2(t, \hbar(t)) \\ f_3(t, \hbar(t)) \\ f_4(t, \hbar(t)) \\ f_5(t, \hbar(t)) \\ f_6(t, \hbar(t)) \end{bmatrix}, $$

Thus, the formulation System (5) can be expressed as follows:

$$ \begin{cases} \mathrm{D}_t^{\mu}\hbar_t = F(t, \hbar(t)), & 0 < \mu \le 1, \\ \hbar(0) = \hbar_0. \end{cases} \tag{6} $$

Lemma 1 provides the solution to (6) only when the right-hand side equals zero:

$$ \hbar(t) + \hbar_0 + XF(t, \hbar(t)) + \bar{X}\int_{0}^{t}F(\xi, \hbar(\Theta))\mathrm{d}\Theta, \tag{7} $$

$$ \text{where } X = \frac{1-\mu}{\kappa(\mu)} \quad \text{and} \quad \bar{X} = \frac{\mu}{\kappa(\mu)}. $$

Now, we proceed to define the Banach space $\mathcal{D} = L[0,T]$ for deeper analysis, establishing the norm of $\mathcal{D} = L[0,T]$ over the interval $0 < t \le T < \infty$:

$$ \|\hbar\| = \sup_{t\in[0,T]}\{|\hbar(t)| : \hbar \in \mathcal{D}\}. $$

4.1 Theorem

(Krassnoselski fixed point theorem) Given a convex and closed subset $\mathcal{D} \subset \mathcal{X}$, there exist two operators $\mathcal{A}$ and $\mathcal{B}$ such that
(1) $\mathcal{A}\hbar_1 + \mathcal{B}\hbar_2 \in \mathcal{D}$;
(2) $\mathcal{B}$ is both continuous and compact, whereas $\mathcal{A}$ represents a contraction.

(3) There exists at least one fixed point $\hbar$ satisfying the equation $\mathcal{A}\hbar + \mathcal{B}\hbar = \hbar$.

The subsequent statement is valid:

($\mathcal{H}1$) Suppose $\mathcal{K}_F > 0$ is a constant, then

$$|F(t, \hbar(t)) - F(t, \overline{\hbar}(t))| \leq \mathcal{K}_F|\hbar - \overline{\hbar}|,$$

($\mathcal{H}2$) When considering the two constants $C_F > 0$ and $\mathcal{M}_F > 0$, it can be observed that

$$|F(t, \hbar)| \leq C_F|\hbar| + \mathcal{M}_F.$$

4.2 Theorem

Due to Theorem 4.1, equation (7) possesses at least one solution if $GF < 1$.

Proof

Suppose we aim to designate set D as a set with compactness and closure properties, $\mathcal{D} = \{\hbar \in \mathcal{X} : ||\hbar|| \leq r\}$. If A and B represent two operators, then:

$$\begin{aligned} \mathcal{A}\hbar(t) &= \hbar_0 + GF(t, \hbar(t)), \\ \mathcal{B}\hbar(t) &= \overline{G}\int_0^t F(\xi, \hbar(\xi))\mathrm{d}\xi. \end{aligned} \tag{8}$$

Regarding the contraction condition of $\mathcal{A}$ as defined in (8), considering $\hbar$ and $\overline{\hbar} \in \mathcal{X}$, it follows that

$$\begin{aligned} ||\mathcal{A}\hbar - \mathcal{A}\overline{\hbar}|| &= \sup_{t\in[0,T]} |\mathcal{A}\hbar(t) - \mathcal{A}\overline{\hbar}(t)| \\ &= \sup_{t\in[0,T]} G|F(t, \hbar(t)) - F(t, \overline{\hbar}(t))| \\ &\leq GF[||\hbar - \overline{\hbar}||]. \end{aligned} \tag{9}$$

Therefore, $\mathcal{A}$ exhibits contraction properties. To assess the compactness of $\mathcal{B}$, contemplate the following:

$$\begin{aligned} |\mathcal{B}\hbar(t)| &= \left|\overline{G}\int_0^t F(\Theta, \hbar(\Theta))\mathrm{d}\Theta\right| \\ &\leq \overline{G}\int_0^t |F(\Theta, \hbar(\Theta))|\mathrm{d}\Theta. \end{aligned} \tag{10}$$

Taking max of (10), we have

$$\begin{aligned} ||\mathcal{B}\hbar|| &\leq \overline{G}\sup_{t\in[0,T]}\int_0^t |F(\Theta, \hbar(\Theta))|\mathrm{d}\Theta \\ &\leq \overline{G}\sup_{t\in[0,T]}\int_0^t [C_F||\hbar|| + \mathcal{M}_F]\mathrm{d}\Theta \\ &\leq \overline{G}T(C_F r + \mathcal{M}_F). \end{aligned} \tag{11}$$

Subsequently, in (11), $\mathcal{B}$ is bounded. Considering the domain of t as $t_1 < t_2$, we derive

$$\begin{aligned} |\mathcal{B}\hbar(t_2) - \mathcal{B}\hbar(t_1)| &= \left|\overline{G}\int_0^{t_2} F(\Theta, \hbar)\mathrm{d}\Theta - \overline{G}\int_0^{t_1} F(\Theta, \hbar)\mathrm{d}\Theta\right| \\ &= \left|\overline{G}\int_0^{t_2} F(\Theta, \hbar)\mathrm{d}\Theta + \overline{G}\int_{t_1}^{0} F(\Theta, \hbar(\Theta))\mathrm{d}\Theta\right| \\ &\leq \overline{G}\int_{t_1}^{t_2} |F(\Theta, \hbar)|\mathrm{d}\Theta \\ &\leq \overline{G}(C_F r + \mathcal{M}_F). \end{aligned} \tag{12}$$

As $t_2 \to t_1$, the right-hand side of (12) approaches zero. Additionally, due to the uniform boundedness of $\mathcal{B}$, $|\mathcal{B}\hbar(t_2) - \mathcal{B}\hbar(t_1)| \to 0$. Consequently, all the conditions specified in Theorem (4.2) are met, establishing the existence of at least one solution to the analyzed model (6) since $\mathcal{B}$ is entirely continuous.

4.3 Theorem

Considering ($\mathcal{H}_1$), when $\overline{G}\mathcal{F}(1 + T) < 1$, it implies that there exists a unique solution to the problem presented in (6). Consequently, multiple solutions exist for Model (2).

Proof

Suppose $\mathcal{P} : \mathcal{X} \to \mathcal{X}$ represents an operator defined as follows:

$$\mathcal{P}\hbar(t) = \hbar_0 + GF(t, \hbar(t)) + \overline{G}\int_0^{t_1} F(\Theta, \hbar(\Theta))\mathrm{d}\Theta.$$

Let $\hbar, \overline{\hbar} \in \mathcal{X}$, then

$$\begin{aligned} ||\mathcal{P}(\hbar) - \mathcal{P}(\overline{\hbar})|| &= \sup_{t\in[0,T]} |\mathcal{P}(\hbar)(t) - \mathcal{P}(\overline{\hbar})(t)| \\ &\leq \sup_{t\in[0,T]} G|F(t, \hbar(t)) - F(t, \overline{\hbar}(t))| \\ &\quad + \overline{G}\sup_{t\in[0,T]}|\int_0^t |(F(\Theta, \hbar(\Theta))) - F(\Theta, (\overline{\hbar}(\Theta)))|\mathrm{d}\Theta \\ &\leq \overline{G}F||\hbar - \overline{\hbar}|| + GFT||\hbar - \overline{\hbar}||. \end{aligned}$$

It suggests that

$$||\mathcal{P}(\hbar(-\mathcal{P}(\overline{\hbar})))|| \leq \overline{G}F(1 + T)||\hbar - \overline{\hbar}||. \tag{13}$$

Therefore, Problem (6) can have a maximum of one solution, signifying that Model (2) possesses a unique solution.

5 Numerical schemes

This section overviews the numerical techniques used to solve the aforementioned model. The Laplace Adomian decomposition (LAD) approach has become more prevalent in engineering and research for tackling complicated issues. The successful resolution of several challenging problems has shown its usefulness. The LAD approach is the primary numerical method used in this work. The conventional Runge–Kutta fourth order (RK4) approach is also used to evaluate the precision and confirm the findings acquired by LAD. It is possible to assess the accuracy and reliability of the LAD methodology by comparing the results of the two approaches.

5.1 Creating a generalized algorithm for solving the model using LADM

We derive a solution as a series by assigning $\kappa(\mu) = 1$ and employing the Laplace transform [54–60]. Consequently, the subsequent algorithm can be formulated as follows:

$$\begin{cases} \dfrac{s\mathcal{L}[W_S(t)] - W_S(0)}{s + \mu(1-s)} = \left[\omega - \omega_2\dfrac{W_A W_S}{N} - \omega_1 W_S\right], \\ \dfrac{s\mathcal{L}[W_E(t)] - W_E(0)}{s + \mu(1-s)} = \left[\omega_2\dfrac{W_A W_S}{N} - (\omega_7 + \omega_1)W_E\right], \\ \dfrac{s\mathcal{L}[W_A(t)] - W_A(0)}{s + \mu(1-s)} = [\omega_7 W_E - (\omega_1 + \omega_3 + \omega_4 + \omega_5)W_A], \\ \dfrac{s\mathcal{L}[W_Q(t)] - W_Q(0)}{s + \mu(1-s)} = [\omega_4 W_A - (\omega_1 + \omega_5 + \omega_6)W_Q], \\ \dfrac{s\mathcal{L}[W_R(t)] - W_R(0)}{s + \mu(1-s)} = [\omega_6 W_Q + \omega_3 W_A - \omega_1 W_R], \\ \dfrac{s\mathcal{L}[W_V(t)] - W_V(0)}{s + \mu(1-s)} = [\omega\eta - \omega_1 W_V]. \end{cases} \tag{14}$$

$$\begin{cases} \mathcal{L}[W_S(t)] = \dfrac{W_S(0)}{s} + \dfrac{s + \mu(1-s)}{s}\left[\omega - \omega_2\dfrac{W_A W_S}{N} - \omega_1 W_S\right], \\ \mathcal{L}[W_E(t)] = \dfrac{W_S(0)}{s} + \dfrac{s + \mu(1-s)}{s}\left[\omega_2\dfrac{W_A W_S}{N} - (\omega_7 + \omega_1)W_E\right], \\ \mathcal{L}[W_A(t)] = \dfrac{W_S(0)}{s} + \dfrac{s + \mu(1-s)}{s}[\omega_7 W_E \\ \qquad - (\omega_1 + \omega_3 + \omega_4 + \omega_5)W_A], \\ \mathcal{L}[W_Q(t)] = \dfrac{W_S(0)}{s} + \dfrac{s + \mu(1-s)}{s}[\omega_4 W_A \\ \qquad - (\omega_1 + \omega_5 + \omega_6)W_Q], \\ \mathcal{L}[W_R(t)] = \dfrac{W_S(0)}{s} + \dfrac{s + \mu(1-s)}{s}[\omega_6 W_Q + \omega_3 W_A - \omega_1 W_R], \\ \mathcal{L}[W_V(t)] = \dfrac{W_S(0)}{s} + \dfrac{s + \mu(1-s)}{s}[\omega\eta - \omega_1 W_V]. \end{cases} \tag{15}$$

Using initial conditions of System (2),

$$\begin{cases} \mathcal{L}[W_S(t)] = \dfrac{P_1}{s} + \dfrac{s + \mu(1-s)}{s}\left[\omega - \omega_2\dfrac{W_A W_S}{N} - \omega_1 W_S\right], \\ \mathcal{L}[W_E(t)] = \dfrac{P_2}{s} + \dfrac{s + \mu(1-s)}{s}\left[\omega_2\dfrac{W_A W_S}{N} - (\omega_7 + \omega_1)W_E\right], \\ \mathcal{L}[W_A(t)] = \dfrac{P_3}{s} + \dfrac{s + \mu(1-s)}{s}[\omega_7 W_E \\ \qquad - (\omega_1 + \omega_3 + \omega_4 + \omega_5)W_A], \\ \mathcal{L}[W_Q(t)] = \dfrac{P_4}{s} + \dfrac{s + \mu(1-s)}{s}[\omega_4 W_A \\ \qquad - (\omega_1 + \omega_5 + \omega_6)W_Q], \\ \mathcal{L}[W_R(t)] = \dfrac{P_5}{s} + \dfrac{s + \mu(1-s)}{s}[\omega_6 W_Q + \omega_3 W_A - \omega_1 W_R], \\ \mathcal{L}[W_V(t)] = \dfrac{P_6}{s} + \dfrac{s + \mu(1-s)}{s}[\omega\eta - \omega_1 W_V]. \end{cases} \tag{16}$$

Let us consider that the solution we compute is in the form of an infinite series:

$$W_S(t) = \sum_{n=0}^{\infty}(W_S)_n(t), \quad W_E(t) = \sum_{n=0}^{\infty}(W_E)_n(t),$$

$$W_A(t) = \sum_{n=0}^{\infty}(W_A)_n(t), \quad W_Q(t) = \sum_{n=0}^{\infty}(W_Q)_n(t),$$

$$W_R(t) = \sum_{n=0}^{\infty}(W_R)_n(t), \quad \text{and} \quad W_V(t) = \sum_{n=0}^{\infty}(W_V)_n(t).$$

The nonlinear term $W_A W_S$ can be expressed in terms of Adomian polynomials as

$$W_A W_S = \sum_{n=0}^{\infty} R_n(t),$$

where

$$R_n = \frac{1}{\Psi(n+1)}\frac{\mathrm{d}^n}{\mathrm{d}\lambda^n}\left[\left(\sum_{k=0}^{n}\lambda^k W_{A,k}\right)\left(\sum_{k=0}^{n}\lambda^k W_{S,k}\right)\right]\Bigg|_{\lambda=o},$$

$$\begin{aligned} n = 0: &\quad R_0 = (W_A)_0(t)(W_S)_0(t), \\ n = 1: &\quad R_1 = (W_A)_0(t)(W_S)_1(t) + (W_A)_1(t)(W_S)_0(t), \\ n = 2: &\quad R_2 = (W_A)_0(t)(W_S)_0(t) + (W_A)_1(t)(W_S)_1(t) \\ &\quad + (W_A)_2(t)(W_S)_0(t), \\ n = 3: &\quad R_3 = (W_A)_0(t)(W_S)_3(t) + (W_A)_1(t)(W_S)_2(t) \\ &\quad + (W_A)_2(t)(W_S)_1(t) + (W_A)_3(t)(W_S)_0(t), \\ n = 4: &\quad R_4 = (W_A)_0(t)(W_S)_4(t) + (W_A)_1(t)(W_S)_3(t) \\ &\quad + (W_A)_2(t)(W_S)_2(t) + (W_A)_3(t)(W_S)_1(t) \\ &\quad + (W_A)_4(t)(W_S)_0(t), \\ &\vdots \\ n = n: &\quad R_n = (W_A)_0(t)(W_S)_n(t) + (W_A)_1(t)(W_S)_{n-1}(t) \\ &\quad + \cdots + (W_A)_{n-1}(t)(W_S)_1(t) + (W_A)_n(t)(W_S)_0(t). \end{aligned}$$

Taking these values into account, the model evolves:

$$
\begin{cases}
\mathcal{L}\left[\sum_{k=0}^{\infty} W_S(t)\right] = \frac{P_1}{s} + \frac{s+\mu(1-s)}{s}\left[\omega - \omega_2\frac{\sum_{k=0}^{\infty}R_k}{N} - \omega_1\sum_{k=0}^{\infty}(W_S)_k\right],\\
\mathcal{L}\left[\sum_{k=0}^{\infty} W_E(t)\right] = \frac{P_2}{s} + \frac{s+\mu(1-s)}{s}\left[\omega_2\frac{\sum_{k=0}^{\infty}R_k}{N} - (\omega_7+\omega_1)\sum_{k=0}^{\infty}(W_E)_k\right],\\
\mathcal{L}\left[\sum_{k=0}^{\infty} W_A(t)\right] = \frac{P_3}{s} + \frac{s+\mu(1-s)}{s}\left[\omega_7\sum_{k=0}^{\infty}(W_E)_k - (\omega_1+\omega_3+\omega_4+\omega_5)\sum_{k=0}^{\infty}(W_A)_k\right],\\
\mathcal{L}\left[\sum_{k=0}^{\infty} W_Q(t)\right] = \frac{P_4}{s} + \frac{s+\mu(1-s)}{s}\left[\omega_4\sum_{k=0}^{\infty}(W_A)_k - (\omega_1+\omega_5+\omega_6)\sum_{k=0}^{\infty}(W_Q)_k\right],\\
\mathcal{L}\left[\sum_{k=0}^{\infty} W_R(t)\right] = \frac{P_5}{s} + \frac{s+\mu(1-s)}{s}\left[\omega_6\sum_{k=0}^{\infty}(W_Q)_k + \omega_3\sum_{k=0}^{\infty}(W_A)_k - \omega_1\sum_{k=0}^{\infty}(W_R)_k\right],\\
\mathcal{L}\left[\sum_{k=0}^{\infty} W_V(t)\right] = \frac{P_6}{s} + \frac{s+\mu(1-s)}{s}\left[\omega\eta - \omega_1\sum_{k=0}^{\infty}(W_V)_k\right].
\end{cases} \tag{17}
$$

Upon comparing the terms in (17), we obtain

Case-1. If $n = 0$, then

$$
\begin{cases}
\mathcal{L}[(W_S)_0(t)] = \frac{P_1}{s} + \frac{s+\mu(1-s)}{s}\mathcal{L}[\omega],\\
\mathcal{L}[(W_E)_0(t)] = \frac{P_2}{s},\\
\mathcal{L}[(W_A)_0(t)] = \frac{P_3}{s},\\
\mathcal{L}[(W_Q)_0(t)] = \frac{P_4}{s},\\
\mathcal{L}[(W_R)_0(t)] = \frac{P_5}{s},\\
\mathcal{L}[(W_V)_0(t)] = \frac{P_6}{s} + \frac{s+\mu(1-s)}{s}\mathcal{L}[\omega\eta].
\end{cases} \tag{18}
$$

Upon performing the inverse Laplace transformation, we acquire

$$
\begin{cases}
(W_S)_0(t) = P_1 + [\omega][1+\mu(t-1)],\\
(W_E)_0(t) = P_2,\\
(W_A)_0(t) = P_3,\\
(W_Q)_0(t) = P_4,\\
(W_R)_0(t) = P_5,\\
(W_V)_0(t) = P_6 + [\omega\eta][1+\mu(t-1)].
\end{cases} \tag{19}
$$

Case-2. If $n = 1$, then

$$
\begin{cases}
\mathcal{L}[(W_S)_1(t)] = \frac{s+\mu(1-s)}{s}\left[-\omega_2\frac{R_0}{N} - \omega_1(W_S)_0\right],\\
\mathcal{L}[(W_E)_1(t)] = \frac{s+\mu(1-s)}{s}\left[\omega_2\frac{R_0}{N} - (\omega_7+\omega_1)(W_E)_0\right],\\
\mathcal{L}[(W_A)_1(t)] = \frac{s+\mu(1-s)}{s}[\omega_7(W_E)_0 - (\omega_1+\omega_3+\omega_4+\omega_5)(W_A)_0],\\
\mathcal{L}[(W_Q)_1(t)] = \frac{s+\mu(1-s)}{s}[\omega_4(W_A)_0 - (\omega_1+\omega_5+\omega_6)(W_Q)_0],\\
\mathcal{L}[(W_R)_1(t)] = \frac{s+\mu(1-s)}{s}[\omega_6(W_Q)_0 + \omega_3(W_A)_0 - \omega_1(W_R)_0],\\
\mathcal{L}[(W_V)_1(t)] = \frac{s+\mu(1-s)}{s}[-\omega_1(W_V)_0].
\end{cases} \tag{20}
$$

Upon performing the inverse Laplace transformation, we acquire

$$
\begin{cases}
(W_S)_1(t) = \left[-\omega_2\frac{(W_A)_0(W_S)_0}{N} - \omega_1(W_S)_0\right][1+\mu(t-1)],\\
(W_E)_1(t) = \left[\omega_2\frac{(W_A)_0(W_S)_0}{N} - (\omega_7+\omega_1)(W_E)_0\right][1+\mu(t-1)],\\
(W_A)_1(t) = [\omega_7(W_E)_0 - (\omega_1+\omega_3+\omega_4+\omega_5)(W_A)_0][1+\mu(t-1)],\\
(W_Q)_1(t) = [\omega_4(W_A)_0 - (\omega_1+\omega_5+\omega_6)(W_Q)_0][1+\mu(t-1)],\\
(W_R)_1(t) = [\omega_6(W_Q)_0 + \omega_3(W_A)_0 - \omega_1(W_R)_0][1+\mu(t-1)],\\
(W_V)_1(t) = [-\omega_1(W_V)_0][1+\mu(t-1)].
\end{cases} \tag{21}
$$

Case-3. If $n = 2$, then

$$
\begin{cases}
\mathcal{L}[(W_S)_2(t)] = \dfrac{s+\mu(1-s)}{s}\left[-\omega_2\dfrac{R_1}{N} - \omega_1(W_S)_1\right], \\
\mathcal{L}[(W_E)_2(t)] = \dfrac{s+\mu(1-s)}{s}\left[\omega_2\dfrac{R_1}{N} - (\omega_7+\omega_1)(W_E)_1\right], \\
\mathcal{L}[(W_A)_2(t)] = \dfrac{s+\mu(1-s)}{s}[\omega_7(W_E)_1 - (\omega_1+\omega_3+\omega_4+\omega_5)(W_A)_1], \\
\mathcal{L}[(W_Q)_2(t)] = \dfrac{s+\mu(1-s)}{s}[\omega_4(W_A)_1 - (\omega_1+\omega_5+\omega_6)(W_Q)_1], \\
\mathcal{L}[(W_R)_2(t)] = \dfrac{s+\mu(1-s)}{s}[\omega_6(W_Q)_1 + \omega_3(W_A)_1 - \omega_1(W_R)_1], \\
\mathcal{L}[(W_V)_2(t)] = \dfrac{s+\mu(1-s)}{s}[-\omega_1(W_V)_1].
\end{cases} \tag{22}
$$

$$
\begin{cases}
\mathcal{L}[(W_S)_2(t)] = \dfrac{s+\mu(1-s)}{s}\left[-\omega_2\dfrac{(W_A)_1(W_S)_1}{N} - \omega_1(W_S)_1\right], \\
\mathcal{L}[(W_E)_2(t)] = \dfrac{s+\mu(1-s)}{s}\left[\omega_2\dfrac{(W_A)_1(W_S)_1}{N} - (\omega_7+\omega_1)(W_E)_1\right], \\
\mathcal{L}[(W_A)_2(t)] = \dfrac{s+\mu(1-s)}{s}[\omega_7(W_E)_1 - (\omega_1+\omega_3+\omega_4+\omega_5)(W_A)_1], \\
\mathcal{L}[(W_Q)_2(t)] = \dfrac{s+\mu(1-s)}{s}[\omega_4(W_A)_1 - (\omega_1+\omega_5+\omega_6)(W_Q)_1], \\
\mathcal{L}[(W_R)_2(t)] = \dfrac{s+\mu(1-s)}{s}[\omega_6(W_Q)_1 + \omega_3(W_A)_1 - \omega_1(W_R)_1], \\
\mathcal{L}[(W_V)_2(t)] = \dfrac{s+\mu(1-s)}{s}[-\omega_1(W_V)_1].
\end{cases} \tag{23}
$$

Upon performing the inverse Laplace transformation, we acquire (Table 1)

$$
\begin{cases}
(W_S)_2(t) = \left[-\omega_2\dfrac{1}{N}(\omega_7(W_E)_0 - (\omega_1+\omega_3+\omega_4+\omega_5)(W_A)_0)\left(-\omega_2\dfrac{(W_A)_0(W_S)_0}{N} - \omega_1(W_S)_0\right) - \omega_1\left(-\omega_2\dfrac{(W_A)_0(W_S)_0}{N} - \omega_1(W_S)_0\right)\right]\left[1+2\mu(t-1)+\mu^2\left(\dfrac{t^2}{2!}-2t+1\right)\right], \\
(W_E)_2(t) = \left[\omega_2\dfrac{1}{N}(\omega_7(W_E)_0 - (\omega_1+\omega_3+\omega_4+\omega_5)(W_A)_0)\left(-\omega_2\dfrac{(W_A)_0(W_S)_0}{N} - \omega_1(W_S)_0\right) - (\omega_7+\omega_1)\left(\omega_2\dfrac{(W_A)_0(W_S)_0}{N} - (\omega_7+\omega_1)(W_E)_0\right)\right]\left[1+2\mu(t-1)+\mu^2\left(\dfrac{t^2}{2!}-2t+1\right)\right], \\
(W_A)_2(t) = \left[\omega_7(\omega_2\dfrac{(W_A)_0(W_S)_0}{N} - (\omega_7+\omega_1)(W_E)_0) - (\omega_1+\omega_3+\omega_4+\omega_5)(\omega_7(W_E)_0 - (\omega_1+\omega_3+\omega_4+\omega_5)(W_A)_0)\right]\left[1+2\mu(t-1)+\mu^2\left(\dfrac{t^2}{2!}-2t+1\right)\right], \\
(W_Q)_2(t) = [\omega_4(\omega_7(W_E)_0 - (\omega_1+\omega_3+\omega_4+\omega_5)(W_A)_0) - (\omega_1+\omega_5+\omega_6)(\omega_4(W_A)_0 - (\omega_1+\omega_5+\omega_6)(W_Q)_0)]\left[1+2\mu(t-1)+\mu^2\left(\dfrac{t^2}{2!}-2t+1\right)\right], \\
(W_R)_2(t) = [\omega_6(\omega_4(W_A)_0 - (\omega_1+\omega_5+\omega_6)(W_Q)_0) + \omega_3(\omega_7(W_E)_0 - (\omega_1+\omega_3+\omega_4+\omega_5)(W_A)_0) - \omega_1(\omega_6(W_Q)_0 + \omega_3(W_A)_0 - \omega_1(W_R)_0)]\left[1+2\mu(t-1)+\mu^2\left(\dfrac{t^2}{2!}-2t+1\right)\right], \\
(W_V)_2(t) = [-\omega_1^2(W_V)_0]\left[1+2\mu(t-1)+\mu^2\left(\dfrac{t^2}{2!}-2t+1\right)\right].
\end{cases} \tag{24}
$$

Table 1: Description of the parameters and their values

Parameter	Description	Values per year	Source
ω	Recruitment rate	29.08	[61]
ω_1	Natural mortality rate	0.00004252912	[61]
ω_2	The rate of recovery through natural immunity for infected individuals	0.088366	[36]
ω_3	The rate of recovery through natural immunity for infected individuals	0.088366	[36]
ω_4	The rate of critical illness among infected individuals	0.5	[36]
ω_5	Monkeypox disease fatality rate	0.003286	[36]
ω_6	The rate of recovery among critically ill individuals	0.036246	[36]
ω_7	The rate at which individuals progress from being exposed to becoming infectious	0.016744	[36]
η	Immunity rate	0.1	[36]

To generate additional terms in the series solution, this technique could be applied. As a result, we derive the solution as:

$$\begin{cases} W_S(t) = (W_S)_0(t) + (W_S)_1(t) + (W_S)_2(t) + \cdots \\ W_E(t) = (W_E)_0(t) + (W_E)_1(t) + (W_E)_2(t) + \cdots \\ W_A(t) = (W_A)_0(t) + (W_A)_1(t) + (W_A)_2(t) + \cdots \\ W_Q(t) = (W_Q)_0(t) + (W_Q)_1(t) + (W_Q)_2(t) + \cdots \\ W_R(t) = (W_R)_0(t) + (W_R)_1(t) + (W_R)_2(t) + \cdots \\ W_V(t) = (W_V)_0(t) + (W_V)_1(t) + (W_V)_2(t) + \cdots \end{cases} \tag{25}$$

6 Discussion

In this study, we present the results obtained from solving System (2) using two different methods: the LADM and the RK4 method. The detailed analysis of the dynamics shown by the monkeypox model when exposed to fractional-order variations is the main emphasis of this section. Our goal is to illuminate the deep consequences of changing the fractional-order and so offer priceless insights into the radical influence on the overall behavior and properties of the model. Additionally, we compare the results of two different methodologies, the LAD technique, and the RK4 approach, in order to further clarify the differences between them. By performing this comparison analysis, we want to identify and assess any differences, resemblances, or new insights that might be discovered using various computational methods to examine the monkeypox model in the context of fractional-order dynamics. The figures presented in this study illustrate the dynamics of monkeypox virus transmission and highlight the significant improvements offered by our novel modeling approach. Figure 1 validates our model with real-time data from Ghana, showing a close alignment between observed and predicted cases. This accuracy is attributed to the incorporation of the Caputo–Fabrizio derivative, which captures memory effects more effectively than traditional models using integer-order derivatives. Figure 2 illustrates the stability regions determined by Krasnoselskii's and Banach's fixed point theorems, ensuring that the model's predictions

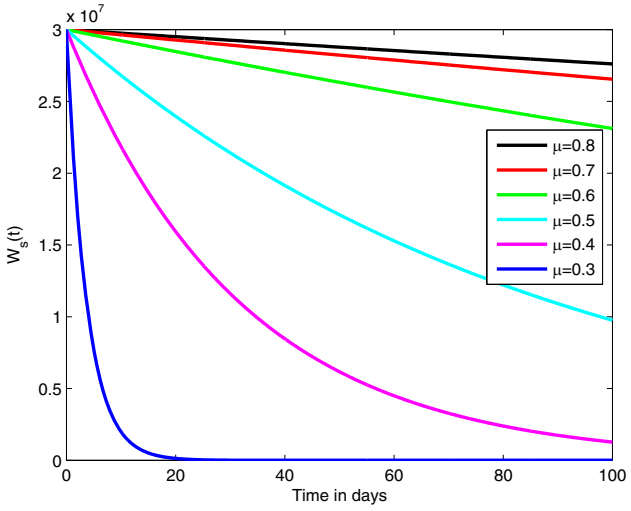

Figure 2: Time series of the susceptible class.

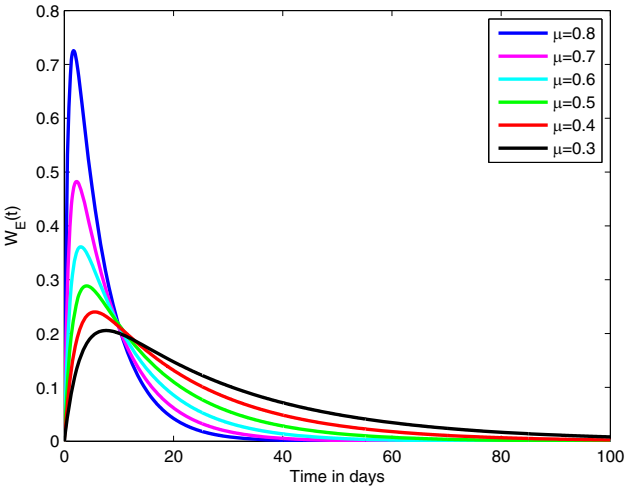

Figure 3: Time series of the exposed class.

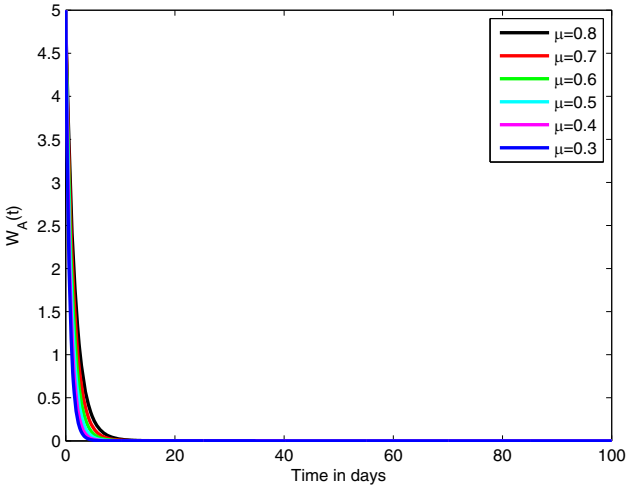

Figure 4: Time series of the infected class.

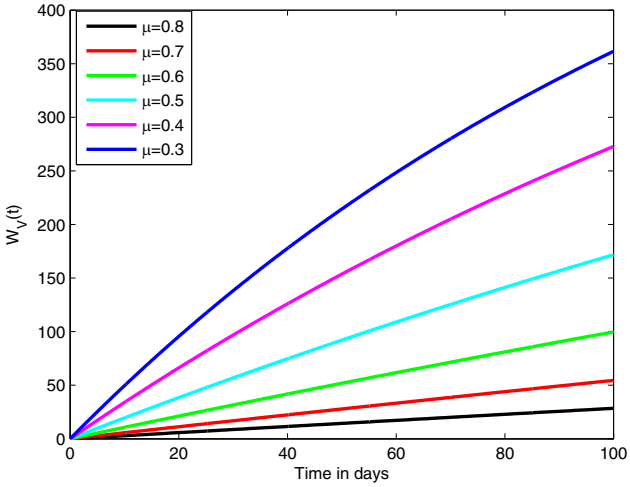

Figure 7: Time series of the immune class.

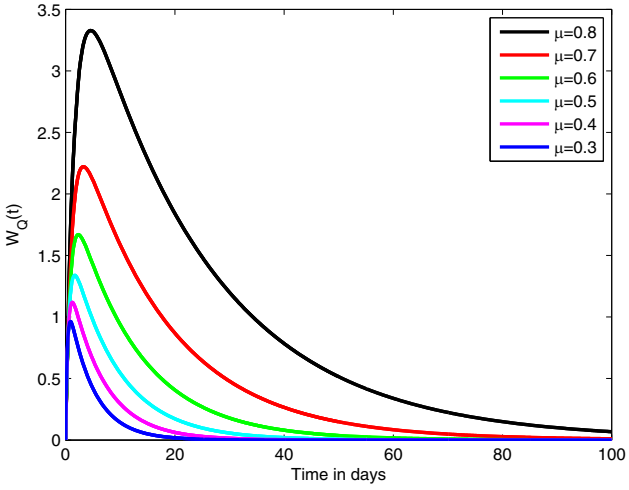

Figure 5: Time series of the hospitalized class.

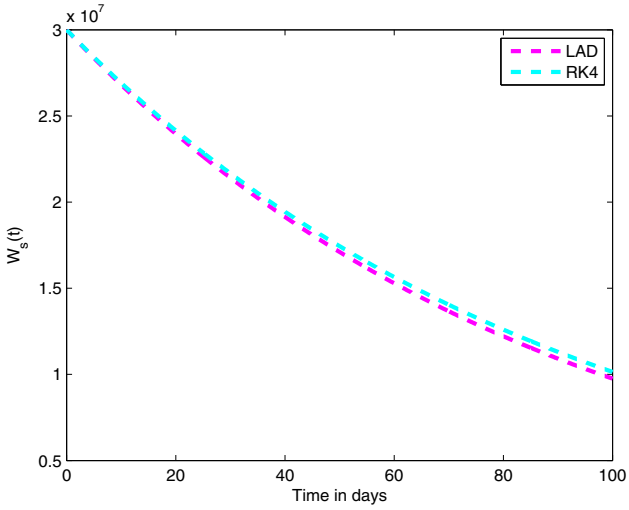

Figure 8: Comparison of the LAD solution for $W_S(t)$ with RK4.

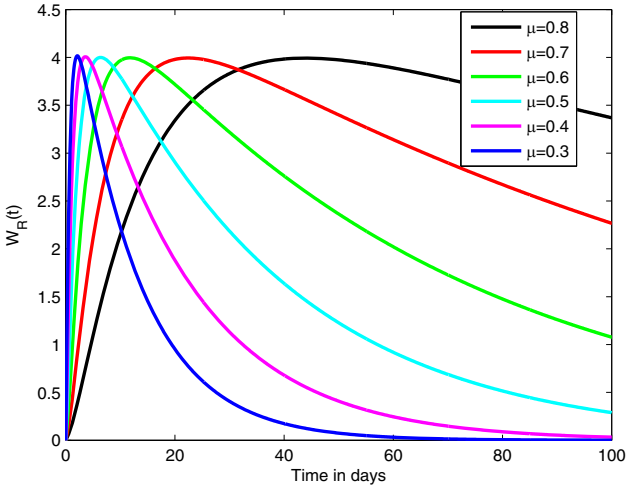

Figure 6: Time series of the recovered class.

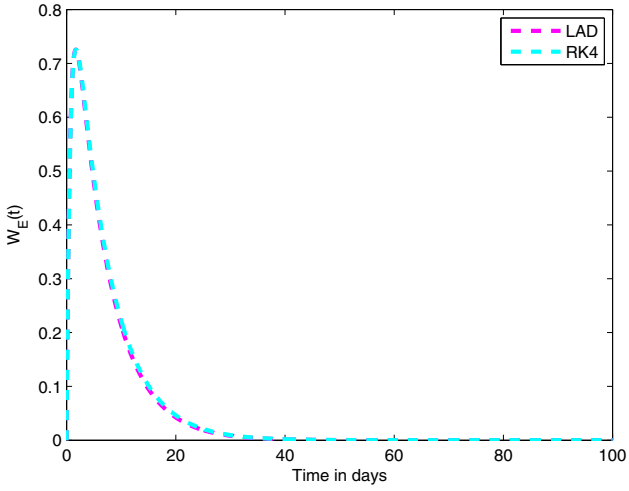

Figure 9: Comparison of the LAD solution for $W_E(t)$ with RK4.

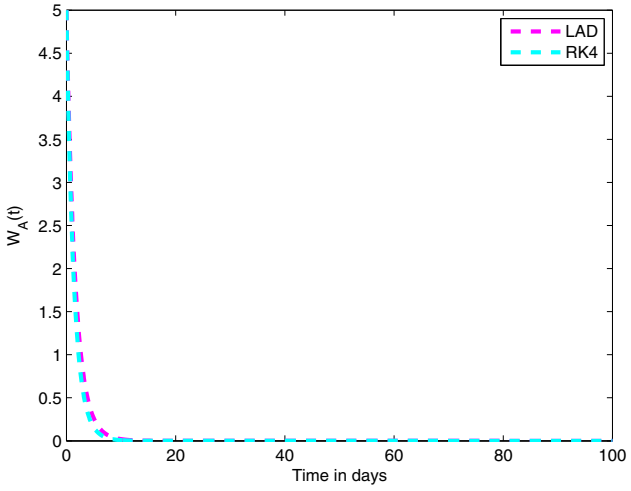

Figure 10: Comparison of the LAD solution for $W_A(t)$ with RK4.

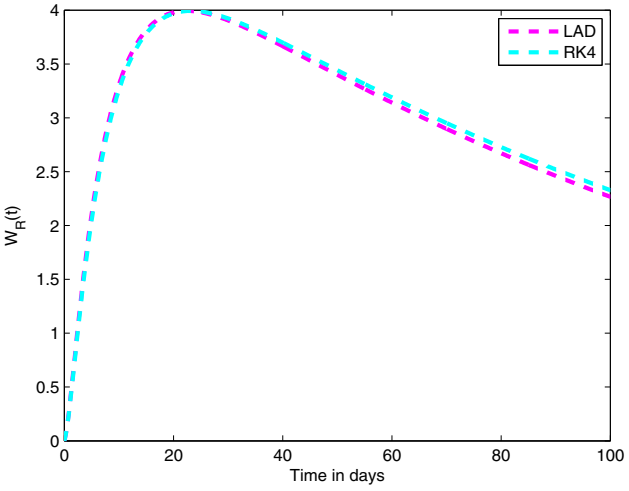

Figure 12: Comparison of the LAD solution for $W_R(t)$ with RK4.

remain consistent and reliable over time. This rigorous stability analysis is often lacking in previous models, leading to less dependable forecasts. Figure 3 compares the approximate solutions obtained from the LADM with those from the RK4 method, showing strong agreement and validating the LADM's accuracy. This demonstrates that our model handles non-linearities efficiently, an improvement over traditional numerical techniques. Figure 4 displays a sensitivity analysis, highlighting the critical parameters influencing disease spread. This nuanced understanding, enabled by fractional calculus, informs more effective public health policies. Overall, these figures demonstrate that our model not only aligns well with real-world data but also offers enhanced accuracy, stability, and practical applicability compared to existing models, contributing to a more robust understanding and control of monkeypox virus transmission. The solutions were computed for six distinct values of the parameter μ in the range of $[0, 1]$, employing a step size of 0.1 over a time span of 100 days. Our analysis reveals a direct correlation between the reduction in the susceptible population and the decrease in the fractional operator μ. Specifically, as the value of μ decreases, we observe an early peak in the number of exposed and hospitalized individuals (Figures 3 and 5) and a rapid decay in the number of infected individuals within the first 5 days (Figure 4). The recovered data exhibit a similar early peak with a decline in the operator value, demonstrating the model's crossover effect (Figure 6). Furthermore, the number of immune individuals increases proportionally with the reduction in the value of μ (Figure 7). To compare the LAD and RK4 solutions, Figures 8–13 depict their respective outcomes. Notably, both methods yield approximately similar results; however, the

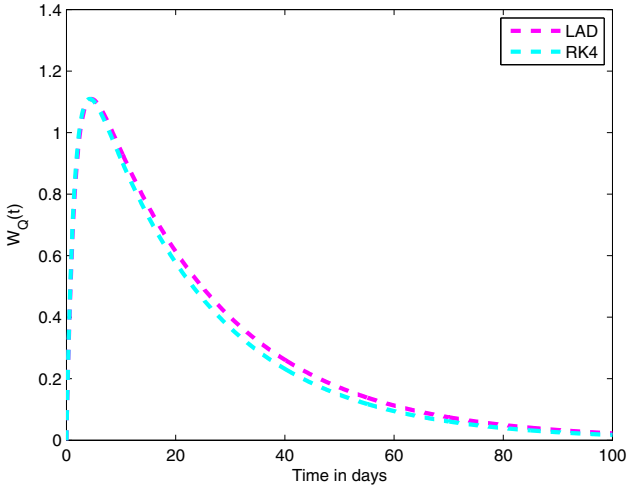

Figure 11: Comparison of the LAD solution for $W_Q(t)$ with RK4.

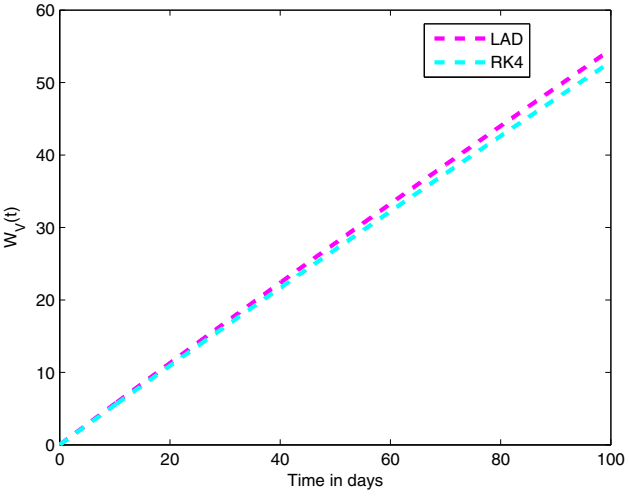

Figure 13: Comparison of the LAD solution for $W_V(t)$ with RK4.

LADM requires more central processing unit time compared to the RK4 method. Overall, the choice between these methods depends on the trade-off between solution accuracy and computational efficiency.

7 Conclusion

This work illuminates monkeypox viral transmission patterns and their public health consequences. In view of a novel mathematical model, we have gained a better understanding of the virus's spread and potential control measures. We analyzed the model's stability qualities using the Caputo–Fabrizio derivative and Krasnoselskii's and Banach's fixed point techniques, laying the groundwork for further research. The model's capacity to capture monkeypox viral transmission patterns was confirmed by Ghana real-time data validation. The LAD has provided vital insights into the system's behaviour, helping us choose control solutions. The LAD and RK4 solutions' individual traits and benefits have allowed us to make educated selections depending on the problem's nature and computational efficiency needs. This study gives policymakers and healthcare practitioners vital tools to reduce monkeypox outbreaks. Analytical and computational methods have helped us handle varied scenarios and overcome this extremely contagious infectious illness. This research offers promise for enhanced infectious disease preparation and response in the face of global public health issues. This mathematical model can inspire multidisciplinary study on monkeypox viral transmission. Scientists, healthcare professionals, and governments must work together to reduce the monkeypox virus's public health effect and protect communities globally. In conclusion, our study opens up several promising avenues for future research in the modeling of infectious disease transmission, particularly concerning monkeypox virus outbreaks. First, further investigation into the long-term dynamics of the disease, including the impact of interventions such as vaccination campaigns and public health measures, could provide valuable insights into disease control strategies. Additionally, exploring the role of spatial heterogeneity and human mobility patterns in disease spread could enhance the accuracy of predictive models. Moreover, incorporating genetic and genomic data into the modeling framework could facilitate a deeper understanding of viral evolution and its implications for disease transmission. Furthermore, the development of real-time forecasting models, coupled with advanced data analytics and machine learning techniques, holds immense potential for early detection and rapid response to outbreaks. Finally, interdisciplinary collaborations between mathematicians, epidemiologists, and public health practitioners are essential for translating research findings into actionable strategies for mitigating the impact of monkeypox virus and other infectious diseases on global health. By addressing these future research directions, we can further advance our understanding of disease dynamics and improve our ability to effectively control and prevent outbreaks.

Acknowledgments: The authors gratefully acknowledge the funding of the Deanship of Graduate Studies and Scientific Research, Jazan University, Saudi Arabia, through project number RG24-S048.

Funding information: The authors gratefully acknowledge the funding of the Deanship of Graduate Studies and Scientific Research, Jazan University, Saudi Arabia, through project number RG24-S048.

Author contributions: All authors have accepted responsibility for the entire content of this manuscript and approved its submission.

Conflict of interest: The authors state no conflict of interest.

References

[1] Haidong Q, Rahman MU, Arfan M. Fractional model of smoking with relapse and harmonic mean type incidence rate under Caputo operator. J Appl Math Comput. 2023;69(1):403–20.
[2] Huntul MJ. Space dependent heat source determination problem with nonlocal periodic boundary conditions. Results Appl Math. 2021;12:100223.
[3] Zhang L, ur Rahman M, Haidong Q, Arfan M. Fractal-fractional Anthroponotic Cutaneous Leishmania model study in sense of Caputo derivative. Alexandr Eng J. 2022;61(6):4423–33.
[4] Alderremy AA, Yasmin H, Shah R, Mahnashi AM, Aly S. Numerical simulation and analysis of Airyas-type equation. Open Phys 2023;21(1):20230144.
[5] Singh M, Tamsir M, El Saman YS, Pundhir S. Approximation of two-dimensional time-fractional Navier-Stokes equations involving Atangana-Baleanu derivative. Int J Math Eng Manag Sci. 2024;9(3):646–67.
[6] Ahmad S, Pak S, Rahman MU, Al-Bossly A. On the analysis of a fractional tuberculosis model with the effect of an imperfect vaccine and exogenous factors under the Mittag-Leffler kernel. Fractal Fract. 2023;7(7):526.
[7] Li B, Wang W, Zhao L, Li M, Yan D, Li X, et al. Aggregation-induced emission-based macrophage-like nanoparticles for targeted photothermal therapy and virus transmission blockage in monkeypox. Adv Materials. 2024;36(9):2305378.
[8] Huntul MJ, Tamsir M. Recovery of timewise-dependent heat source for hyperbolic PDE from an integral condition. Math Meth Appl Sci. 2021;44:1470–83.

[9] Alderremy AA, Gomez-Aguilar JF, Aly S, Saad KM. A fuzzy fractional model of coronavirus (COVID-19) and its study with Legendre spectral method. Results Phys. 2021;21:103773.
[10] Singh M. Approximation of the time-fractional Klein-Gordon equation using the integral and projected differential transform methods. Int J Math Eng Manag Sci. 2023;8(4):672–87.
[11] Khan AA, Amin R, Ullah S, Sumelka W, Altanji M. Numerical simulation of a Caputo fractional epidemic model for the novel coronavirus with the impact of environmental transmission. Alexandr Eng J. 2022;61(7):5083–95.
[12] Kumar S, Ahmadian A, Kumar R, Kumar D, Singh J, Baleanu D, et al. An efficient numerical method for fractional SIR epidemic model of infectious disease by using Bernstein wavelets. Mathematics. 2020;8(4):558.
[13] Abdo MS, Shah K, Wahash HA, Panchal SK. On a comprehensive model of the novel coronavirus (COVID-19) under Mittag-Leffler derivative. Chaos Solitons Fractals. 2020;135:109867.
[14] Zhou Y, Zhang Y. Noether symmetries for fractional generalized Birkhoffian systems in terms of classical and combined Caputo derivatives. Acta Mech. 2020;231(7):3017–29.
[15] Liu X, Dai B, Chuai Y, Hu M, Zhang H. Associations between vitamin D levels and periodontal attachment loss. Clin Oral Invest. 2023;27(8):4727–33.
[16] Chuai Y, Dai B, Liu X, Hu M, Wang Y, Zhang H. Association of vitamin K, fibre intake and progression of periodontal attachment loss in American adults. BMC Oral Health. 2023;23(1):303.
[17] Wang Z, Sun W, Hua R, Wang Y, Li Y, Zhang H. Promising dawn in tumor microenvironment therapy: engineering oral bacteria. Int J Oral Sci. 2024;16(1):24.
[18] Zhang W, Zhang Y, Jin C, Fang R, Hua R, Zang X, et al. The indicative role of inflammatory index in the progression of periodontal attachment loss. Europ J Med Res. 2023;28(1):287.
[19] Wang Y, Wu W, Christelle M, Sun M, Wen Z, Lin Y, et al. Automated localization of mandibular landmarks in the construction of mandibular median sagittal plane. Europ J Med Res. 2024;29(1):84.
[20] UK Health Security Agency. Monkeypox cases confirmed in England-latest updates. 2022.
[21] World Health Organization. Multi-country monkeypox outbreak: situation update. 2022.
[22] Mathieu E, Spooner F, Dattani S, Ritchie H, Roser M. Mpox (monkeypox). Our World in Data. 2022.
[23] Vivancos R, Anderson C, Blomquist P, Balasegaram S, Bell A, Bishop L, et al. Community transmission of monkeypox in the United Kingdom, April to May 2022. Eurosurveillance. 2022;27(22):2200422.
[24] Yinka-Ogunleye A, Aruna O, Dalhat M, Ogoina D, McCollum A, Disu Y, et al. Outbreak of human monkeypox in Nigeria in 2017–18: a clinical and epidemiological report. Lancet Infect Diseases. 2019;19(8):872–9.
[25] Hobson G, Adamson J, Adler H, Firth R, Gould S, Houlihan C, et al. Family cluster of three cases of monkeypox imported from Nigeria to the United Kingdom, May 2021. Eurosurveillance. 2021;26(32):2100745.
[26] Harris E. What to know about monkeypox. Jama. 2022;327(23):2278–9.
[27] Reynolds MG, Doty JB, McCollum AM, Olson VA, Nakazawa Y. Monkeypox re-emergence in Africa: a call to expand the concept and practice of one health. Expert Rev Anti-infective Therapy. 2019;17(2):129–39.
[28] Durski KN, McCollum AM, Nakazawa Y, Petersen BW, Reynolds MG, Briand S, et al. Emergence of monkeypox-west and central Africa, 1970–2017. Morbidity Mortality Weekly Report. 2018;67(10):306.
[29] Usman S, Adamu II. Modeling the transmission dynamics of the monkeypox virus infection with treatment and vaccination interventions. J Appl Math Phys. 2017;5(12):2335.
[30] Reed KD, Melski JW, Graham MB, Regnery RL, Sotir MJ, Wegner MV, et al. The detection of monkeypox in humans in the Western Hemisphere. New England J Med. 2004;350(4):342–50.
[31] Grant R, Nguyen LBL, Breban R. Modelling human-to-human transmission of monkeypox. Bullet World Health Organ. 2020;98(9):638.
[32] Vaughan A, Aarons E, Astbury J, Brooks T, Chand M, Flegg P, et al. Human-to-human transmission of monkeypox virus, United Kingdom, October 2018. Emerging Infect Diseases. 2020;26(4):782.
[33] Nolen LD, Osadebe L, Katomba J, Likofata J, Mukadi D, Monroe B, et al. Extended human-to-human transmission during a monkeypox outbreak in the Democratic Republic of the Congo. Emerg Infect Diseases. 2016;22(6):1014.
[34] Thornhill JP, Barkati S, Walmsley S, Rockstroh J, Antinori A, Harrison LB, et al. Monkeypox virus infection in humans across 16 countries-April-June 2022. New England J Med. 2022;387(8):679–91.
[35] Adadi P, Mensah EO, Abdul-Razak S. The outbreak of monkeypox (MPX) in Ghana. J Med Virol. 2023;95(1):e28171.
[36] Peter OJ, Oguntolu FA, Ojo MM, Olayinka Oyeniyi A, Jan R, Khan I. Fractional order mathematical model of monkeypox transmission dynamics. Phys Scr. 2022;97(8):084005.
[37] Somma SA, Akinwande NI, Chado UD. A mathematical model of monkey pox virus transmission dynamics. IFE J Sci. 2019;21(1):195–204.
[38] Peter OJ, Kumar S, Kumari N, Oguntolu FA, Oshinubi K, Musa R. Transmission dynamics of Monkeypox virus: a mathematical modeling approach. Model Earth Syst Environ. 2022;8:3423–34.
[39] Kalezhi J, Chibuluma M, Chembe C, Chama V, Lungo F, Kunda D. Modelling Covid-19 infections in Zambia using data mining techniques. Results Eng. 2022;13:100363.
[40] Saha S, Bhattacharjee A. A 2D FSI mathematical model of blood flow to analyze the hyper-viscous effects in atherosclerotic COVID patients. Results Eng. 2021;12:100275.
[41] Mohanty B, Costantino V, Narain J, Chughtai AA, Das A, MacIntyre CR. Modelling the impact of a smallpox attack in India and influence of disease control measures. BMJ open. 2020;10(12):e038480.
[42] Bacaër N, Bacaër N. Daniel Bernoulli, d Alembert and the inoculation of smallpox (1760). A short history of mathematical population dynamics. London: Springer; 2011. p. 21–30.
[43] Meltzer MI, Damon I, LeDuc JW, Millar JD. Modeling potential responses to smallpox as a bioterrorist weapon. Emerg Infect Diseases. 2001;7(6):959.
[44] Madaki YU, Manu HA, Gwani AA, Edeghagba EE. Application of mathematical modeling on the spread of chicken pox disease (A case study of Nayinawa clinic Damaturu, Yobe state). Scholars 2020;7:260–71.
[45] Qureshi S, Yusuf A. Modeling chickenpox disease with fractional derivatives: From Caputo to Atangana-Baleanu. Chaos Solitons Fractals. 2019;122:111–8.
[46] Johnson RF, Yellayi S, Cann JA, Johnson A, Smith AL, Paragas J, et al. Cowpox virus infection of cynomolgus macaques as a model of hemorrhagic smallpox. Virology. 2011;418(2):102–12.

[47] Acay B, Inc M, Khan A, Yusuf A. Fractional methicillin-resistant Staphylococcus aureus infection model under Caputo operator. J Appl Math Comput. 2021;67(1):755–83.
[48] Yusuf A, Acay B, Mustapha UT, Inc M, Baleanu D. Mathematical modeling of pine wilt disease with Caputo fractional operator. Chaos Solitons Fractals. 2021;143:110569.
[49] Inc M, Acay B, Berhe HW, Yusuf A, Khan A, Yao SW. Analysis of novel fractional COVID-19 model with real-life data application. Results Phys. 2021;23:103968.
[50] Singh M, Msmali AH, Tamsir M, Ahmadini AAH. An analytical approach of multi-dimensional Navier-Stokes equation in the framework of natural transform. AIMS Math. 2024;9(4):8776–802.
[51] Rahman MU, Ahmad S, Matoog RT, Alshehri NA, Khan T. Study on the mathematical modeling of COVID-19 with Caputo-Fabrizio operator. Chaos Solitons Fractals. 2021;150:111121.
[52] Syafruddin S, Noorani MSM. SEIR model for transmission of dengue fever in Selangor Malaysia. Int J Modern Phys Conference Series. 2012;9:380–9.
[53] Derouich M, Boutayeb A, Twizell EH. A model of dengue fever. Biomedical Eng Online. 2003;2(1):1–10.
[54] Shah R, Khan H, Baleanu D. Fractional Whitham-Broer-Kaup equations within modified analytical approaches. Axioms. 2019;8(4):125.
[55] Botmart T, Agarwal RP, Naeem M, Khan A. On the solution of fractional modified Boussinesq and approximate long wave equations with non-singular kernel operators. AIMS Math. 2022;7:12483–513.
[56] Al-Sawalha MM, Khan A, Ababneh OY, Botmart T. Fractional view analysis of Kersten-Krasilashchik coupled KdV-mKdV systems with non-singular kernel derivatives. AIMS Math. 2022;7(10):18334–59.
[57] Alderremy AA, Shah R, Iqbal N, Aly S, Nonlaopon K. Fractional series solution construction for nonlinear fractional reaction-diffusion Brusselator model utilizing Laplace residual power series. Symmetry. 2022;14(9):1944.
[58] Alshammari S, Al-Sawalha MM, Shah R. Approximate analytical methods for a fractional-order nonlinear system of Jaulent-Miodek equation with energy-dependent Schrodinger potential. Fractal Fract. 2023;7(2):140.
[59] Alqhtani M, Saad KM, Shah R, Hamanah WM. Discovering novel soliton solutions for (3+1)-modified fractional Zakharov-Kuznetsov equation in electrical engineering through an analytical approach. Opt Quantum Electron. 2023;55(13):1149.
[60] Aljahdaly NH, Shah R, Agarwal RP, Botmart T. The analysis of the fractional-order system of third-order KdV equation within different operators. Alexandr Eng J. 2022;61(12):11825–34.
[61] Okyere S, Ackora-Prah J. A mathematical model of transmission dynamics of SARS-CoV-2 (COVID-19) with an underlying condition of diabetes. Int J Math Math Sci. 2022;2022:1–15.